Monitoring Uranium Transformations Determined by the Evolution of Biogeochemical Processes

Terence L. Marsh
Michigan State University

Our contribution to the larger project (ANL) was the phylogenetic analysis of evolved communities capable of reducing metals including uranium. We previously reported structural shifts in microbial communities of microcosms constructed with inocula from uranium-contaminated sediment from the Field Research Center (FRC). Incubations were for up to eleven months and samples were taken from both the top and bottom of the sediment of duplicate microcosms incubated at room temperature anaerobically. The biological indices of the microcosm bacterial communities revealed that under strong selective force (e.g., sulfate and uranium) some populations became dominant and the community diversity appeared reduced. With the reduction of U(VI), bacterial community diversity appeared to recovere to its T0 level. Our clone library results revealed that some bacterial populations were persistent in the microcosms during the 11 month incubation period, while others became more abundant or less detectable in response to the prevailing environmental factors. According to the Ribosomal Database Project's (RDP) *Classifier* tool, *beta-Proteobacteria* and *Acidobacteria* (e.g., *Gp8*) were highly abundant in the microcosms throughout the incubation period, whereas *Desulfovibrio*, a known sulfate-reducing Genus within which uranium reducing capabilities also reside, was substantially more abundant at early sampling times when sulfate and uranium were abundant, compared to at the end of the incubation period (11 months). We speculate that the decrease in abundance of *Desulfovibrio* with time was caused by consumption of sulfate and uranium during early stages of incubation. Interestingly, groups identified by the RDP as unclassified bacteria and unclassified *Desulfobacteraceae* responded to the selective forces differently. These two groups appeared to be more robust at the end of the incubation period when the strong initial selective force of sulfate and uranium was absent or diminished. The statistical community comparison with UniFrac indicated that early and late stage samples were evolved from the original inoculum. The RDP library comparison tool revealed that bacterial community populations shifted at statistically significant amounts according to time and space. For example, as mentioned above, early stage *Desulfovibrio* and *Desulfobacteraceae* abundances were significantly different from those where found at late incubation stage ($P=0.01$). Similarly, iron-oxidizing bacterium *Thiobacillus* was significantly more abundant at late sampling times. These results, combined with data from our colleagues were submitted to and accepted for publication in Environmental Science & Technology [1].

Additional work on this has focused on microcosms that were established several years ago. These were plastic bottles containing sediment from ORNL and spiked with various substrates as shown below. The microcosms were incubated in an anaerobic chamber with 5% H2 and 95% N2 for two years.

M10 = Microcosm 10 (+3 mM sulfate, no ethanol)
M11 = Microcosm 11 (+3 mM sulfate, +3 mM ethanol)
M13 = Microcosm 13 (+9 mM sulfate, no ethanol)
M15 = Microcosm 15 (+9 mM sulfate, +3 mM ethanol)

These samples were then dissected in the following manner. The head water was removed from each microcosm and filtered. The filter retentate DNA was extracted for microbial community analysis. Sediment samples were taken to permit community analysis of the visible differences detected in the microcosms. The top of the sediments were black in comparison to the remaining sediment that was gray. Because we suspected that hydrogen diffusion across the plastic bottle may have contributed to community metabolism, we sampled the "near edge" of the container. Thus there were a total of 5 samples processed for each microcosm, the fluid on top (F), the black surface layer of the sediment (B), the gray sediment below (G), a vertical homogenate of the sediment that is a mixture of both black and gray with gray predominating (VH) and the near edge of the vessel (NE). Figure 9 shows a cartoon of these microcosms.

Community analyses of these samples were carried out in duplicate using DNA extracted with a commercial kit. The results are summarized in the dendrogram constructed from the Bray-Curtis analysis of community phylogenetic profiles (Figure 10) and the distribution of phylotypes is presented in Figures 11-13. The primary environmental attribute that distinguishes the samples is sediment versus head-water. The secondary distinguishing attribute is the black top sediment sample with the ethanol concentration defining the groups within the black sediments. Below the black sediments the sulfate concentration defined community similarities. These sediment communities were delineated first on the basis of sulfate concentration and then on location within the microcosm. Ethanol influenced community structure at both low and high concentrations of sulfate, in both cases selecting for *Geobacter* populations.

In the low sulfate microcosms ethanol drove the grouping of the G and VH samples. The M10 samples had a large abundance of *Sulfuritalea* ranging from 42.5% to 48.2%. The M11 G samples ranged from 30.4% to 33.6% whereas the VH1 samples ranged from 19.0% to 19.2%. In addition *Anaeromyxobacter* was a major contributor at an average of 18.2% and 16.5% for M10 and M11 respectively. In contrast, the abundance of *Geobacter* was much different between the two microcosms with an average of 2.9% and 30.1% for M10 and M11 respectively, indicating that ethanol selected for Geobacter populations. The NE samples at low sufate grouped separately from the rest of the samples. The M10 NE samples had nearly an equal amount of *Sulfuritalea* and *Anaeromyxobacter* averaging 22.5% and 21.2% respectively whereas the M11 NE samples were dominated by *Geobacter* at

an average of 53.2% and to a lesser extent by *Anaeromyxobacter* at 22.2% with *Sulfuritalea* at 10.1%.

Within the high sulfate microcosms ethanol's influence was not as well defined. Ethanol did unambiguously drive the grouping of the NE and VH samples. The M13 NE and VH samples had similar distributions consisting of a large abundance of *Sulfuritalea* at 48.7% and to a lesser extent *Anaeromyxobacter* and *Nitrosospira* at 16.4% and 10.4% respectively. The M15 NE and VH samples were dominated by *Geobacter* at 59.2% and 37.1% respectively. These samples saw a drop in *Sulfuritalea*, *Anaeromyxobacter*, and *Nitrosospira* to an average of 15.0%, 12.1% and 4.4% respectively. The biggest difference separating M15's NE and VH samples was due to *Desulfurivibrio* (3.1% and 20.1% respectively). Interestingly, the M15 G samples were found to be more similar to the M13 VH and NE samples than the M13 G samples were. The M15 G samples were more similar to these VH and NE samples due to *Desulfovibrio* and *Desulfurivibrio;* these G samples had an average of 5.5% and 4.1% respectively, while these NE and VH averaged 7.0% and 3.7% respectively. The M13 G samples averaged only 1.1% and 1.2% for these two genera respectively.

As mentioned previously the B and F samples clustered independently from the other samples. While sulfate was undoubtedly a selection factor it was not as great as the constraints of pelagic growth or more subtle factors. Ethanol determine the clustering of these samples over sulfate. The richness of these four samples was nearly identical. M11_B and M15_B each had a large portion of *Geobacter* both at 71.1%, *Anaeromyxobacter* at 18.3% and 15.2%, and *Desulfvibrio* at 4.9% and 5.4% respectively. What differentiated the two was that *Desulfomonile* was found at an average of 3.1% in M15_B and only at 0.1% in M11_B. The non-ethanol B samples (M10 and M13) grouped together based on the same three genera *Desulfurivibrio*, *Desulfovibrio*, and *Desulfomonile* albeit at different proportions. *Desulfurivibrio* was at an average of 35.6% and 23.2%, *Desulfovibrio* at 21.3% and 36.2%, and *Desulfomonile* at 11.3% and 12.1% for M10 and M13 respectively. M10 also had a larger quantity of *Ignavibacterium*, 6.5% compared to 1.8% in M13. The F samples were outliers compared to the other locations. As seen in the B samples the F samples grouped independently from sulfate and more so based on ethanol content. The M10 and M13 grouping were both based on two dominant genera *Desulfovibrio* and *Desulfomonile* even though the quantity of these genera were much different between the two. *Desulfovibrio* at 20.7% and 87.8%, and *Desulfomonile* at 70.8% and 8.7% for M10 and M13 respectively. The ethanol F samples both consisted of a single dominant genus, *Ignavibacterium* at 76.9% in M11 and *Desulfomonile* at 66.8% in M15. The only similarity between these two samples was *Desulfovibrio* at 9.8% and 20.1% for M11 and M15 respectively.

Trends: *Desulfurivibrio*, *Desulfovibrio*, and *Desulfomonile* are more dominant in sulfate independent groupings (B and F). *Geobacter* more abundant in ethanol samples with the exception of the head-water samples.

We continue to analyze these data from the four microcosms in preparation for writing a paper.

Papers published.

1. **Kelly SD, Kemner KM, Carley J, Criddle C, Jardine PM, Marsh TL, Phillips D, Watson D, Wu WM. 2008**. Speciation of uranium in sediments before and after in situ biostimulation. Environ Sci Technol. 42(5):1558-64.
2. **Kelly SD, Wu WM, Yang F, Criddle CS, Marsh TL, et al. (2010)** Uranium transformations in static microcosms. Environ Sci Technol 44: 236-242**.**

Summary of Figures.

Figure 1. **Phylogenetic distribution at phylum level for clone libraries of all microcosm samples.**

Figure 2. **Bacterial community distribution at genera level in all microcosm samples.**

Figure 3. **Clone library comparisons (at phyla level) of T0 sample and microcosm 1 and 2 samples by using *Libcompare* (RDP tool).**

Figure 4. Demographic shifts of bacterial communities over time and space.

Figure 5. Principal component analysis (PCA) of all microcosm samples.

Figure 6. Clustering (Bray-Curtis) of all microcosm samples revealed grouping similar to PCA plot with the exception that sample T5_Bottom2 clustered closer to the 4°C sample.

Figure 7. Changes of OTU's in microcosms during anaerobic incubation.

Figure 8. Rarefaction curves of clone libraries from microcosm samples showed partial coverage of the bacterial community at 97% similarity.

Figure 9. Image of ANL Microcosms incubated under anaerobic conditions in a chamber with 5% H_2 and 95% N_2. Microcosms were incubated for 1.5 years.

Figure 10. Bray-Curtis relationships of microbial community structures from microcosm samples.

Figure 11. Phylogenetic distribution of bacterial populations from microcosms M10 and M11 including the near edge, vertical homogenate, and gray sediments.

Figure 12. Phylogenetic distribution of bacterial populations from Microcosms M13 and M15 including the near edge, vertical homogenate, and gray sediments.

Figure 13. Phylogenetic distribution of bacterial populations from Microcosms 10, 11, 13 & 15 including the black top sediment (B) and head-water (F) samples.

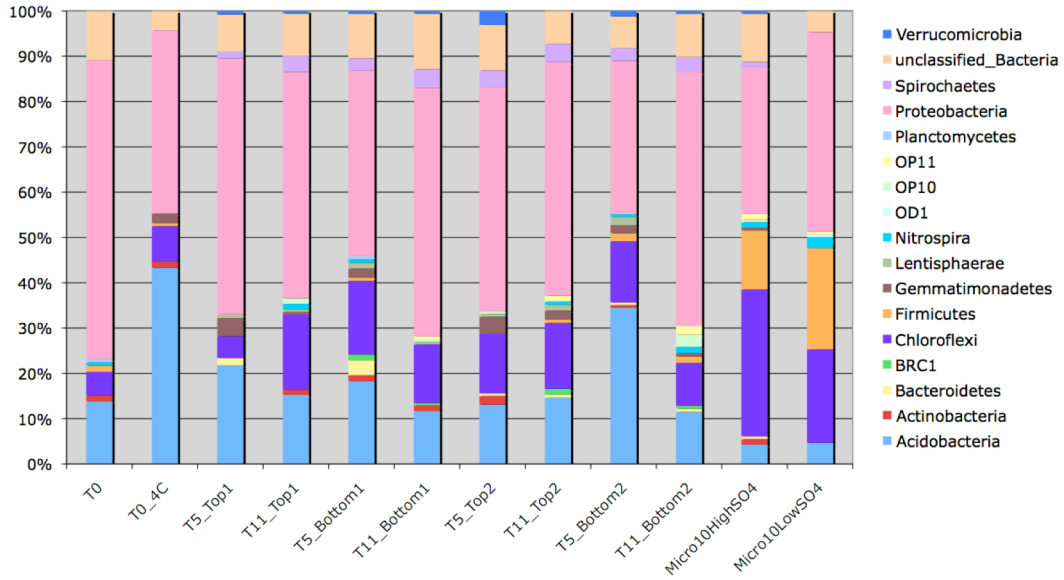

Figure 1. **Phylogenetic distribution at phylum level for clone libraries of all microcosm samples.** Initial soil sediment material (T0) was dispensed into two microcosms (1 and 2). Aqueous (Top) and sediment (Bottom) samples were taken after incubating anaerobically for 5 months (T5) and 11 months (T11) from each microcosm. Sample T0_4C represents the original sediment inoculum that was stored at 4ºC for 11 months while the microcosms were incubated at room temperature. Samples labeled Top or Bottom were taken from the top or bottom of the sediment. T5_Top1 is the top sediment of microcosm 1 at 5 months while T5_Top2 is the top sediment of microcosm 2 at 5 months. Samples labeled T11 were from the eleventh month of incubation. The initial inocula (Micro10-High-SO_4 and Micro10-Low-SO_4) for a new microcosm study were analyzed as well.

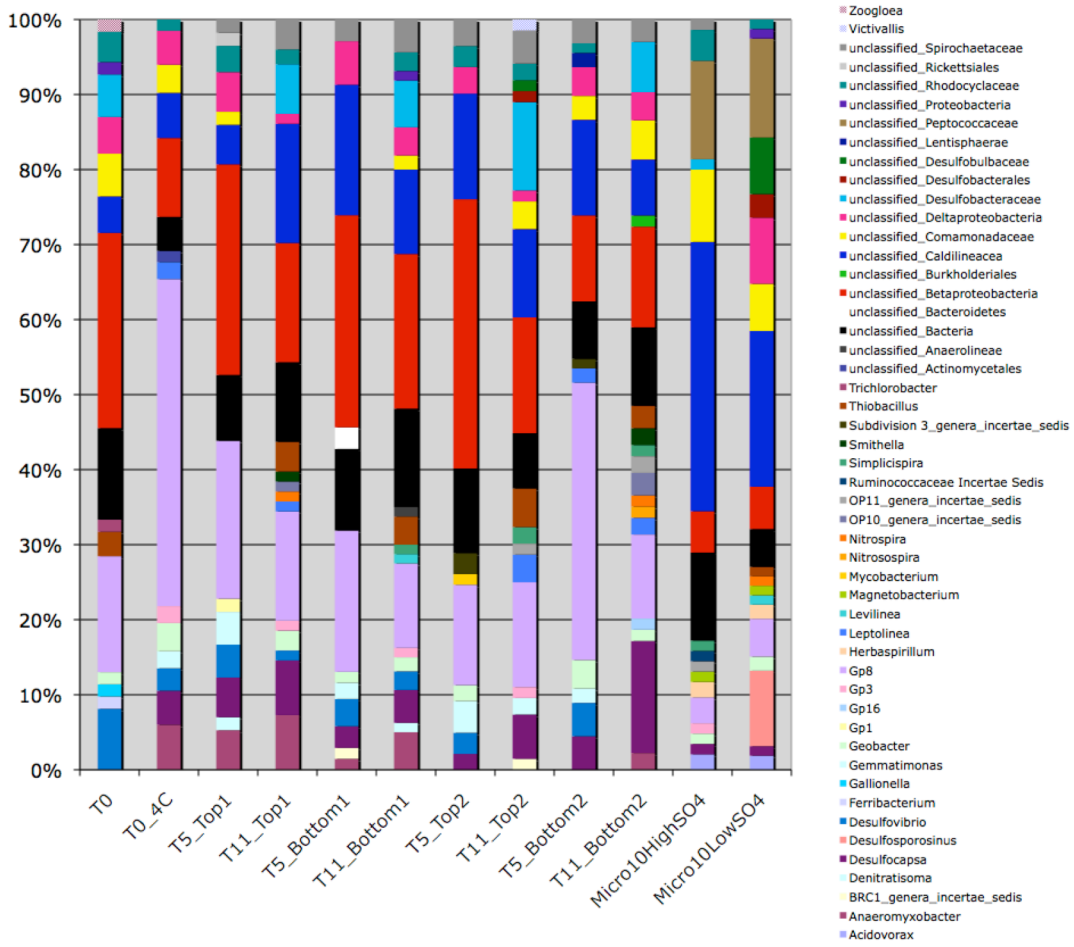

Figure 2. **Bacterial community distribution at genera level in all microcosm samples.** Sample T0_4C represents the original sediment inoculum that was stored at 4ºC for 11 months while the microcosms were incubated at room temperature. Samples labeled Top or Bottom were taken from the top or bottom of the sediment. T5_Top1 is the top sediment of microcosm 1 at 5 months while T5_Top2 is the top sediment of microcosm 2 at 5 months. Samples labeled T11 were from the eleventh month of incubation. The initial inocula (Micro10-High-SO_4 and Micro10-Low-SO_4) for a new microcosm study were analyzed as well.

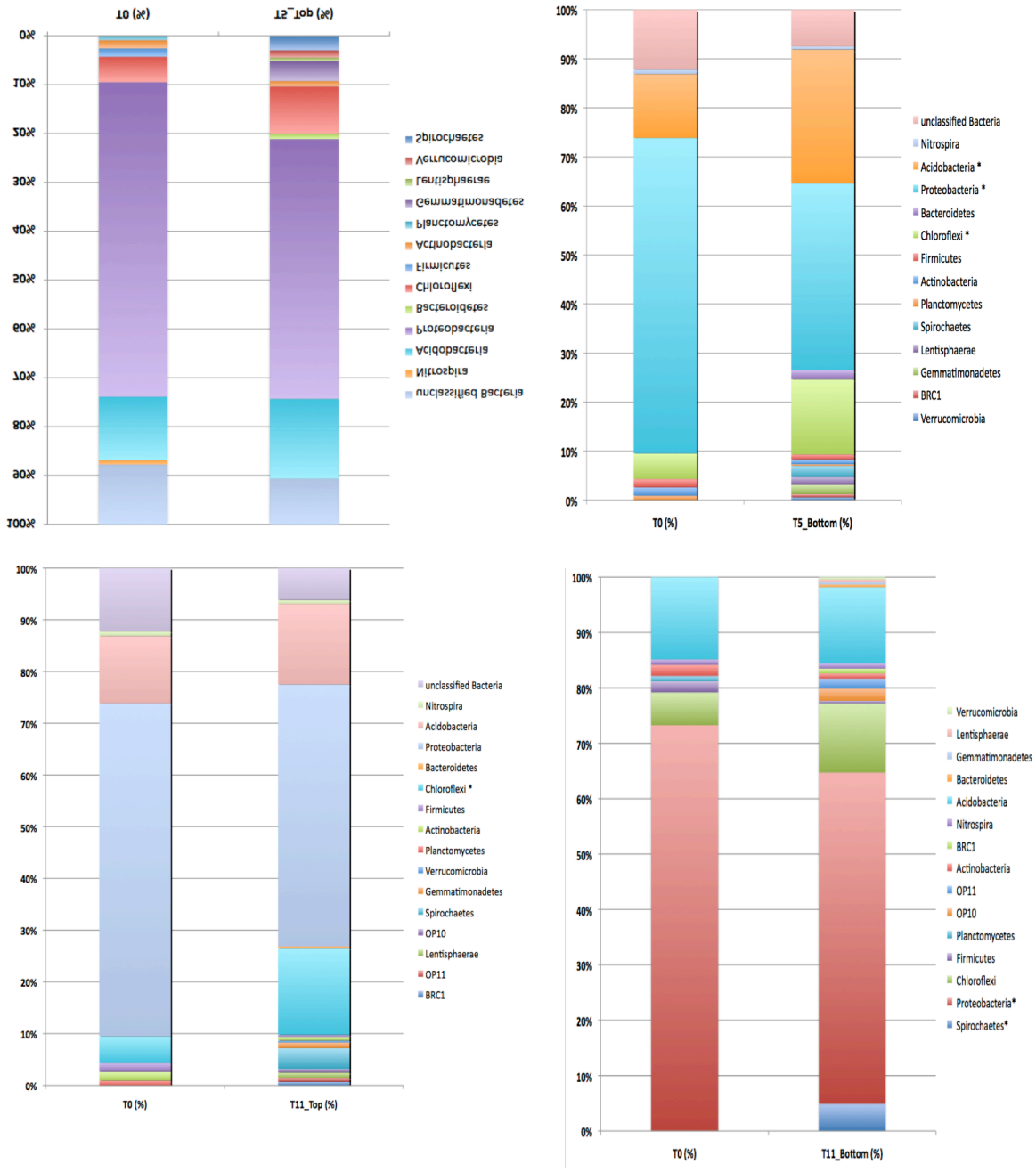

Figure 3. **Clone library comparisons (at phyla level) of T0 sample and microcosm 1 and 2 samples by using *Libcompare* (RDP tool).** DNA sequences from samples collected from microsom 1 and 2 at the same time and depth were pooled together, yielding four composite samples (T5_Top, T5_Bottom, T11_Top and T11_Bottom). Significant changes are denoted by an asterisk. No significant differences were observed between T0 and T5_Top. However, *Acidobacteria* and *Chloroflexi* became significantly more abundant in T5_Bottom than T0. In contrast, the *Proteobacteria* were more abundant in T0. After 11 months of incubation, significant increases of *Chloroflexi* were observed in the aqueous layer of the micrososms. Phylum *Spirochaetes* was significantly more abundant in T11_Bottom than T0 samples.

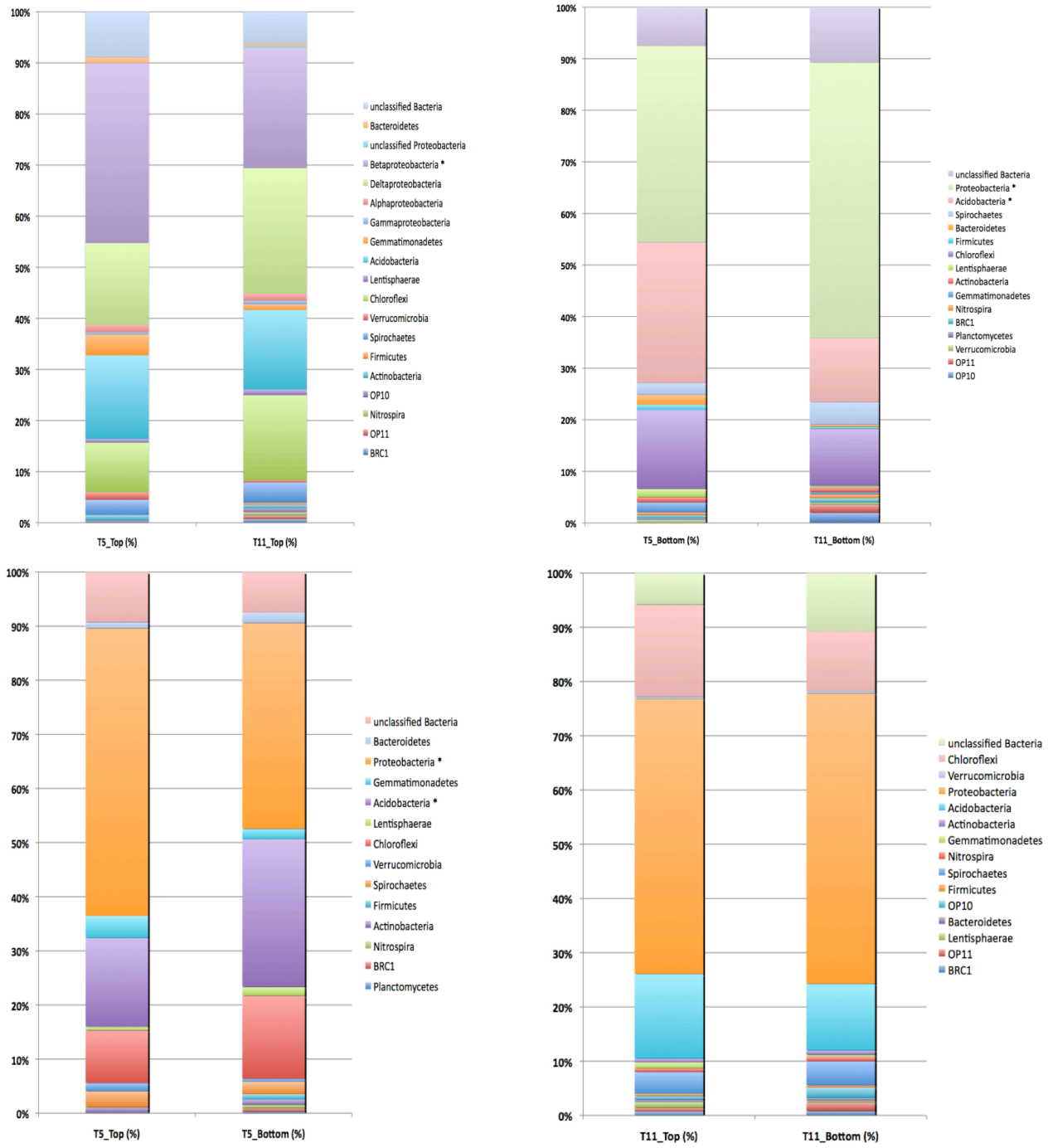

Figure 4. Demographic shifts of bacterial communities over time and space. *Libcompare* (RDP)

revealed that *Betaproteobacteria* decreased significantly in the top layers of sediment during incubation. In the bottom layers, *Proteobacteria* increased significantly while *Acidobacteria* decreased during incubation. Interestingly, fewer *Proteobacteria* but more *Acidobacteria* were detected in the sediment layer of the microcosms at T5 (5months). No significant differences were observed in the top and bottom layers of the microcosms at T11 (11 months).

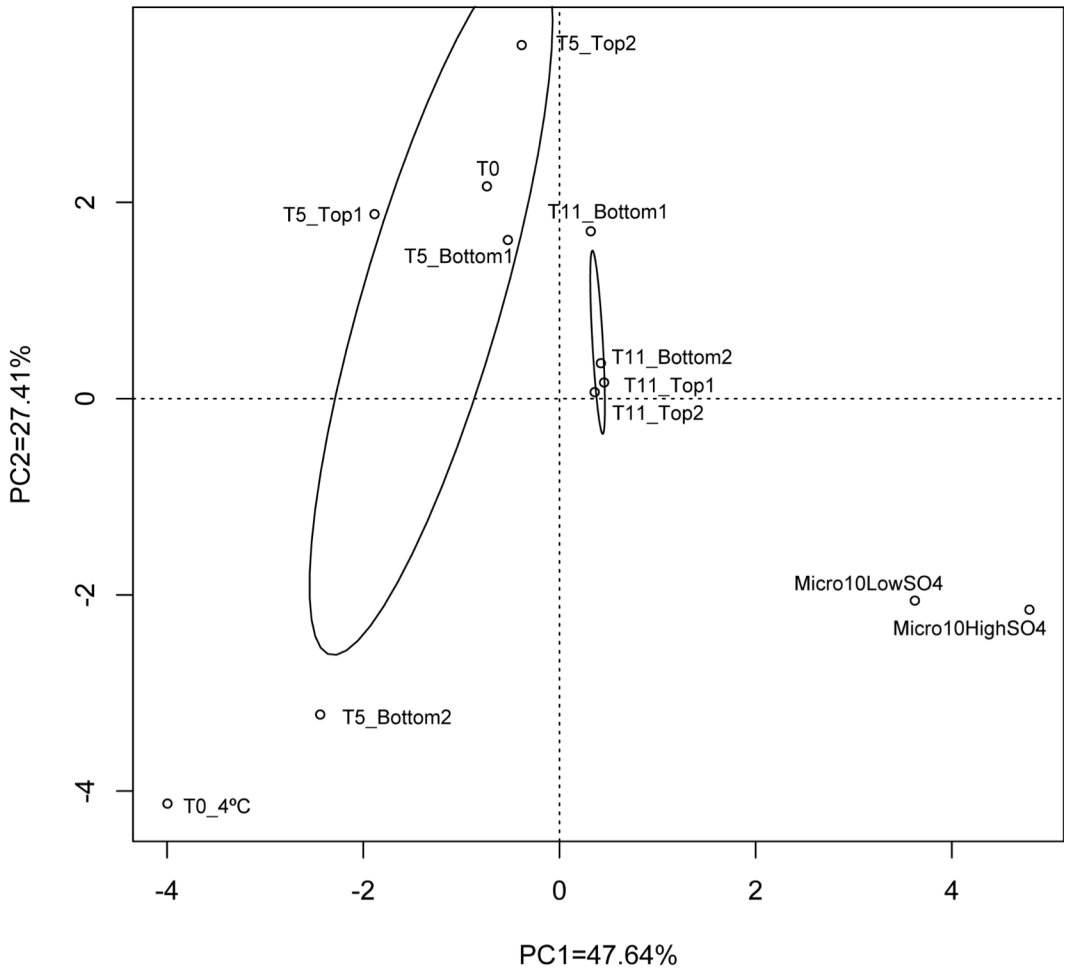

Figure 5. Principal component analysis (PCA) of all microcosm samples. The ellipses were drawn around each group centroid (T5 and T11) at 95% confidence. The PCA plot revealed that bacterial communities were highly variable at T5 (large ellipse, 5 months). However, communities converged significantly at T11 (small ellipse, 11 months) after all uranium was reduced. T0 is included and has similarities to T5 and T11 communities. The inocula of the new microcosm study (low and high SO_4) were significantly different as was the sample incubated at 4°C for 11 months.

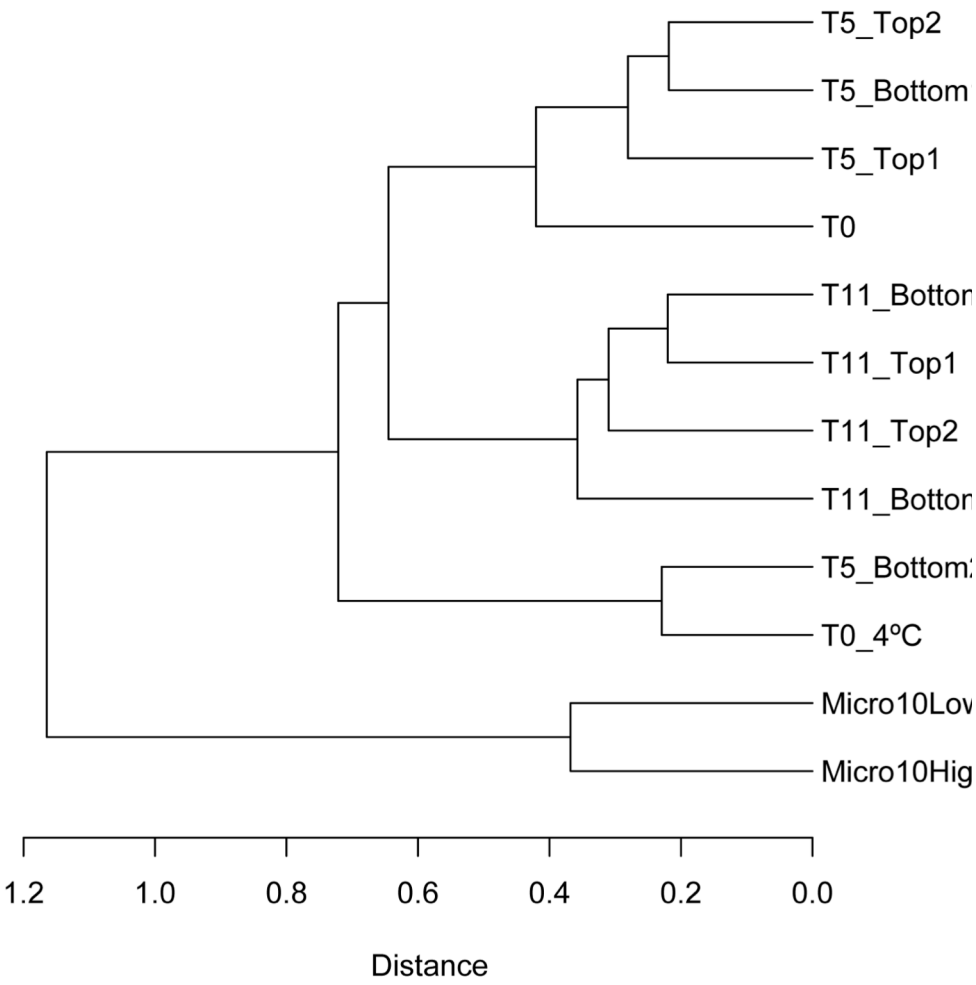

Figure 6. Clustering (Bray-Curtis) of all microcosm samples revealed grouping similar to PCA plot with the exception that sample T5_Bottom2 clustered closer to the 4°C sample.

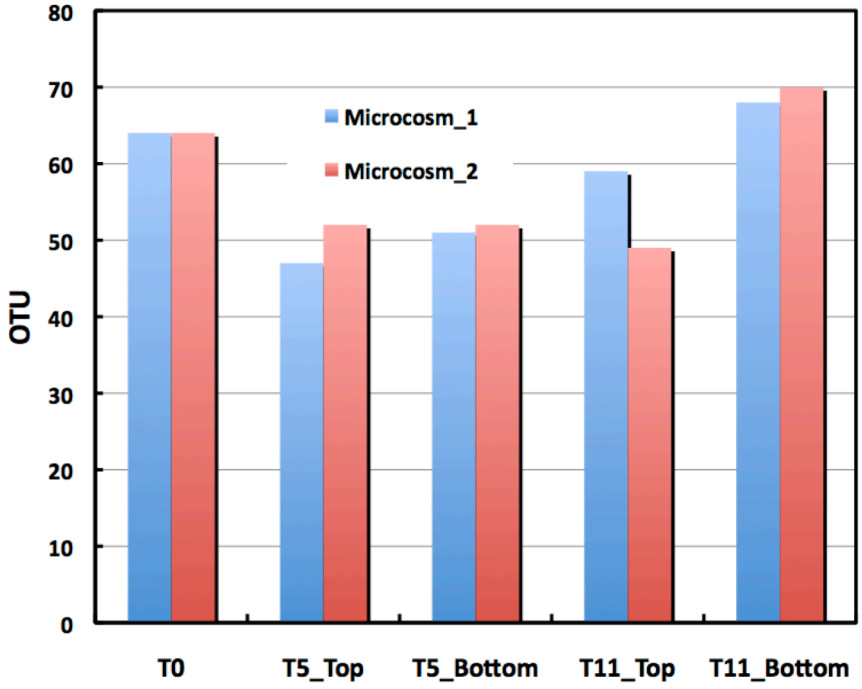

Figure 7. Changes of OTU's in microcosms during anaerobic incubation.

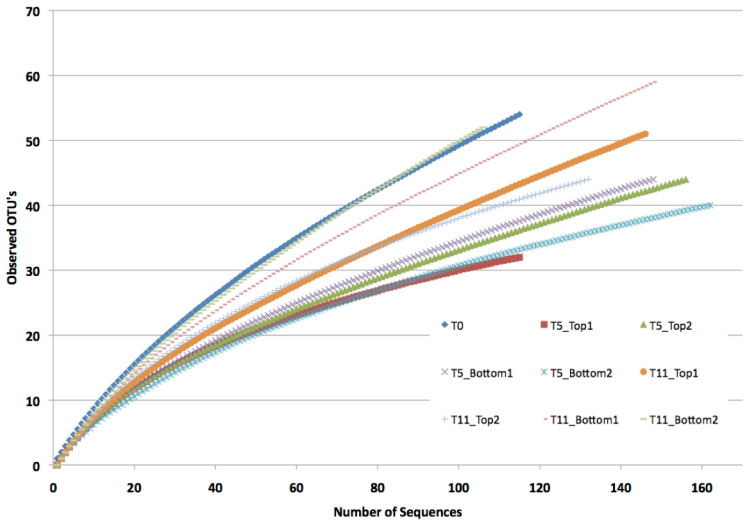

Figure 8. Rarefaction curves of clone libraries from microcosm samples showed partial coverage of the bacterial community at 97% similarity.

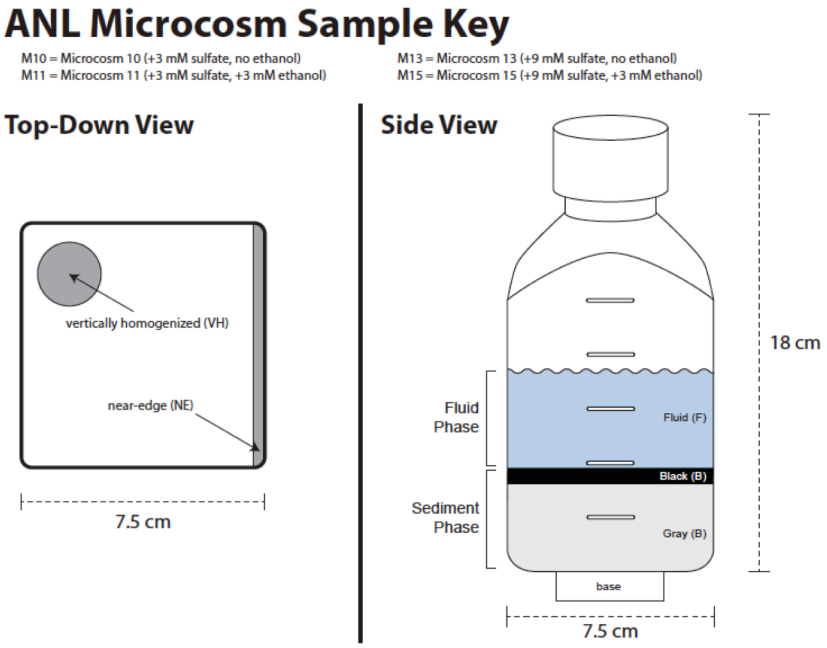

Figure 9. Microcosm structure including details of sampling. Each microcosm was sampled along the near edge (NR), vertically through the sediment (VH), from the fluid phase (F), from the black top of the sediment (B), and from the lower gray part of the sediment.

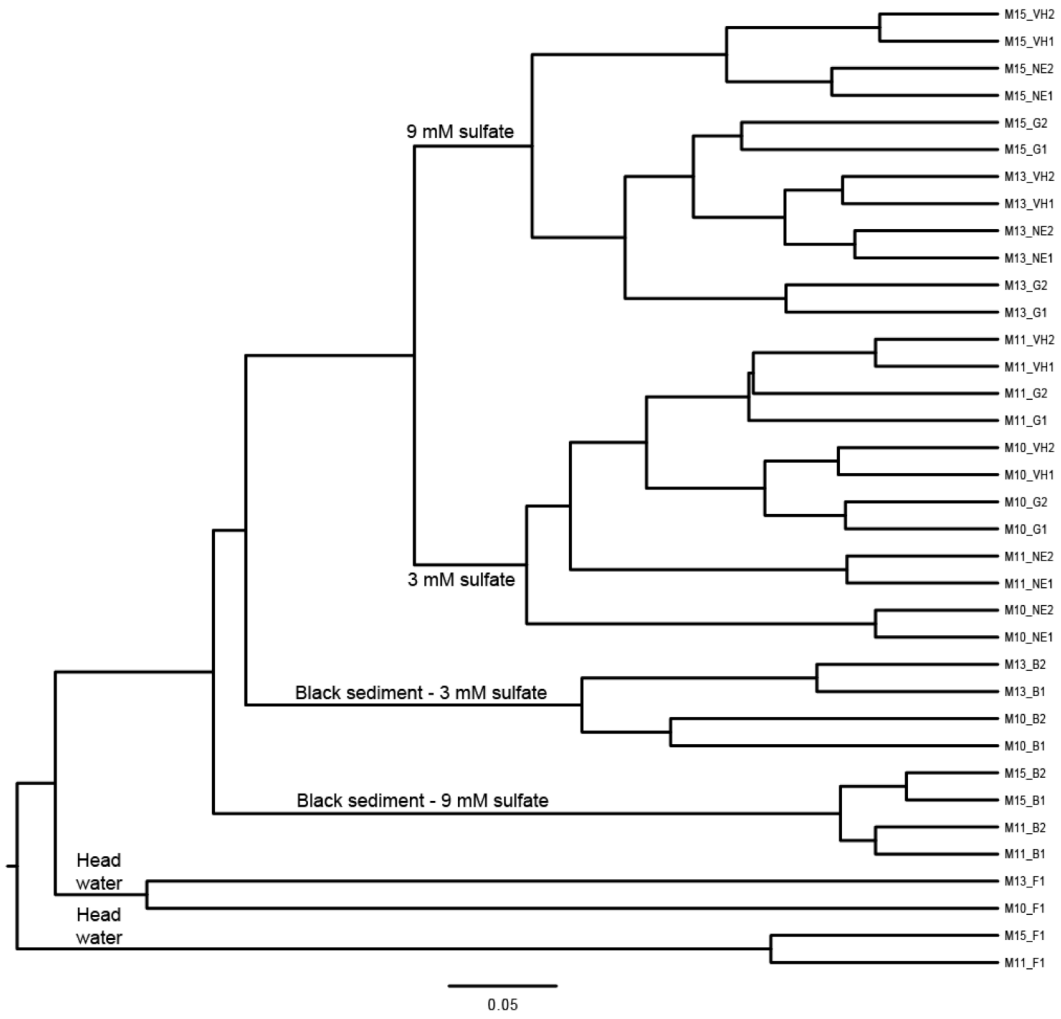

Figure 10. Bray-Curtis relationships of microbial community structures from microcosm samples.

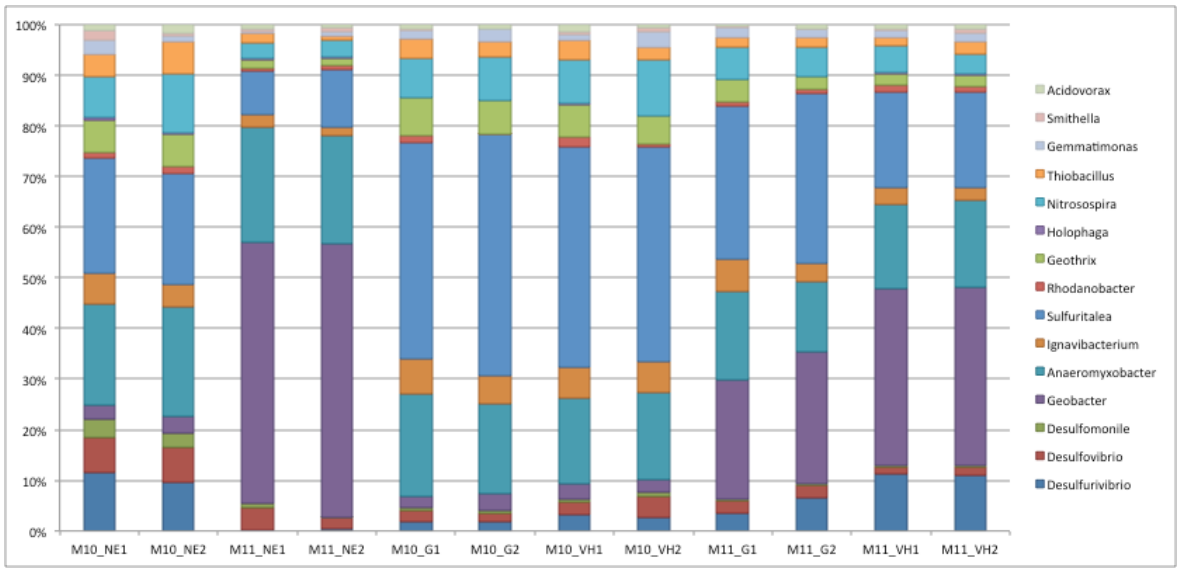

Figure 11. Phylogenetic distribution of bacterial populations from microcosms M10 and M11 including the near edge, vertical homogenate, and gray sediments.

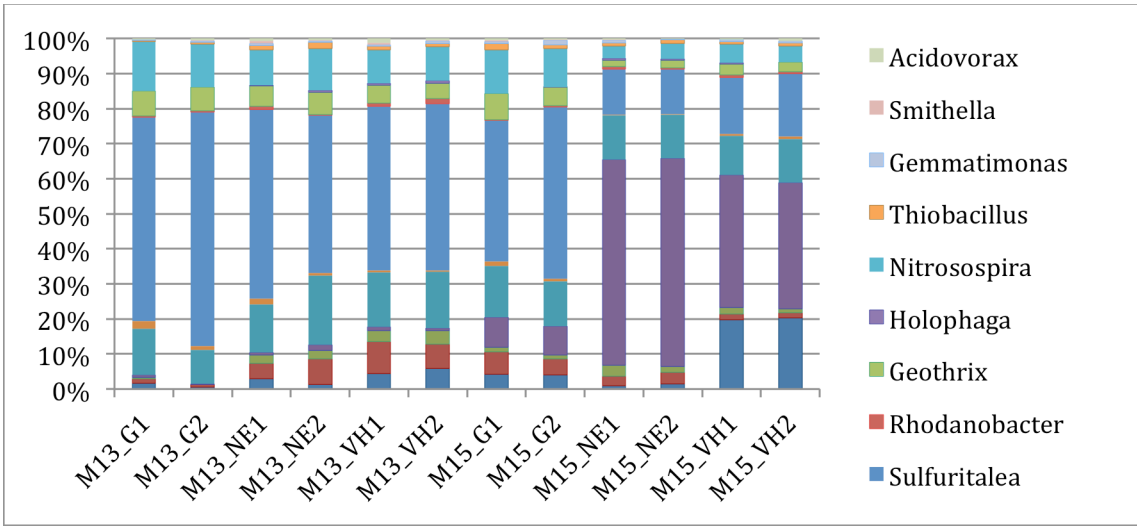

Figure 12. Phylogenetic distribution of bacterial populations from Microcosms M13 and M15 including the near edge, vertical homogenate, and gray sediments.

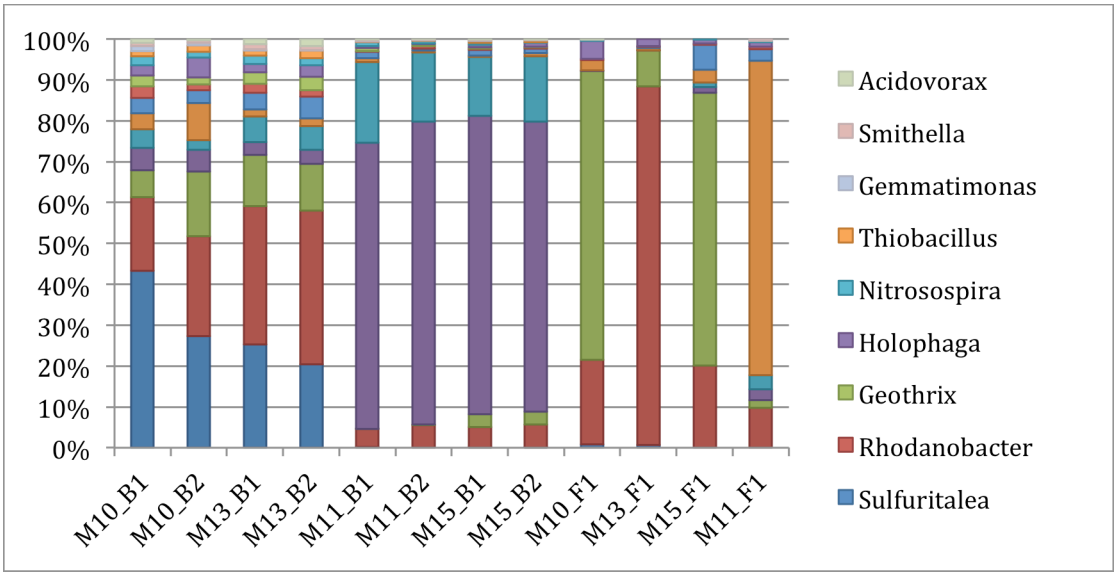

Figure 13. Phylogenetic distribution of bacterial populations from Microcosms 10, 11, 13 & 15 including the black top sediment (B) and head-water (F) samples.